A Novel Series of the New Visible-Light-Driven Photocatalysts $MCo_{1/3}Nb_{2/3}O_3$ (M = Ca, Sr, and Ba) with Special Electronic Structures

Jiang Yin,*,† Zhigang Zou,‡ and Jinhua Ye†,§

Ecomaterials Center, National Institute for Materials Science (NIMS), 1-2-1 Sengen, Tsukuba, Ibaraki 305-0047, Japan, Photoreaction Control Research Center (PCRC), National Institute of Advanced Industrial Science and Technology (AIST), 1-1-1 Higashi, Tsukuba, Ibaraki 305-8565, Japan, and Precursory Research for Embryonic Science and Technology, Japan Science and Technology Corporation (JST), Japan

Received: January 14, 2003; In Final Form: April 1, 2003

A new series of ABO_3-type perovskite photocatalysts $MCo_{1/3}Nb_{2/3}O_3$ (M = Ca, Sr, and Ba) were synthesized by a solid-state reaction method, in which the B site is occupied by Co^{2+} and Nb^{5+} randomly in a charge-balanced manner. They were characterized by powder X-ray diffraction, UV−vis diffuse reflectance spectroscopy and photocatalytic activity measurements with Pt and NiO_x cocatalyst under visible-light irradiation ($\lambda > 420$ nm), respectively. It is determined from the reflectance spectra that the optical transitions for these compounds, corresponding to visible-light absorption, are directly forbidden, and the band structures are suggested to be composed of the Co^{2+} 3d states and the Nb^{5+} 4d states. The feature of the electronic structure for $BaCo_{1/3}Nb_{2/3}O_3$ calculated by the full potential-linearized augmented plane wave (F-LAPW) method shows that the O 2p states are strongly hybridized with the Co^{2+} 3d states, and little hybridized with the Nb^{5+} 4d states. The difference in their photocatalytic activity is ascribed to their special crystal and electronic structures.

1. Introduction

In the past three decades, the semiconductor photocatalyst has received much interest due to its favorable prospects for the conversion of solar energy to chemical energy stored in gaseous hydrogen, anti-fog of motor window, self-cleaning of the construction materials, air-purification in a common space, and environment-organic-pollutant purification, etc.[1−3] Many materials have been found to show high photocatalytic activity under UV light irradiation such as TiO_2 and $Sr_2(Nb,Ta)_2O_7$,[4,5] etc. It is believed that the valence band of the transition metal oxide with a d^0 electronic configuration is composed of an O 2p level and the conduction band is composed of a d level. For the wide-band gap semiconductor TiO_2 ($E_g \sim 3.0$ eV), the conduction band is just above the potential of H^+/H_2, while the top of the valence band (O 2p) is more than 1 eV below the potential of O_2/H_2O. In the case of Ta_2O_5, the valence band (O 2p) is about 2 eV below the potential of O_2/H_2O. So it is suggested to make a new valence band instead of O 2p to develop a new visible-light-response photocatalyst. Recently, $TiO_{2-x}N_x$ and Ta_3N_5 have been shown response to visible-light irradiation.[2,6] In this paper, we report a new series of the visible-light-driven photocatalysts $MCo_{1/3}Nb_{2/3}O_3$ (M = Ca, Sr, and Ba) with ABO_3-type perovskite structure, in which the B site is occupied by Co^{2+} and Nb^{5+} ions randomly in the charge-balanced manner. The electronic structure of $BaCo_{1/3}Nb_{2/3}O_3$ is investigated by using the F-LAPW method.

* Corresponding author.
† National Institute for Materials Science (NIMS).
‡ National Institute of Advanced Industrial Science and Technology (AIST).
§ Japan Science and Technology Corporation (JST).

2. Experimental Section

The polycrystalline powders of $MCo_{1/3}Nb_{2/3}O_3$ (M = Ca, Sr, and Ba) were synthesized by a solid-state reaction method. The starting materials, including $CaCO_3$, $SrCO_3$, $BaCO_3$, CoO, and Nb_2O_5 with high purity and in chemical stoichiometric ratio, were ground and mixed thoroughly, then preheated at 850 °C for 8 h. The preheated mixtures were reground, and finally sintered at 1230 °C for 48 h. The crystal structures of the powder samples were determined by X-ray diffraction (JEOL JDX-3500, Tokyo, Japan). UV−vis diffuse reflectance spectra of these powder samples were measured by using an UV−vis spectrometer (Shimadsu UV-2500PC, Tokyo, Japan). The photocatalytic reactions were examined using a closed gas circulation system. A 300 W Xe arc lamp, a 420 nm cutoff filter, and a Pyrex cell were employed. The gas formation rates were determined with a TCD gas chromatograph (Shimadsu GC-8A, Tokyo, Japan) connected to the system with a circulating line. An H_2 evolution reaction was performed in a CH_3OH/H_2O solution with 0.2 wt % Pt cocatalyst (cat.:0.5 g, Pt: 0.2 wt %, CH_3OH: 50 mL, H_2O: 220 mL), and an O_2 evolution reaction was performed in $AgNO_3$ solution without any cocatalyst (cat.: 0.5 g, $AgNO_3$: 5 mmol, H_2O: 270 mL). In all the experiments, the photocatalyst particles were suspended in solution by stirring with a magnetic stirrer, and the rotative velocity of the stirrer was set at 500 rpm. To introduce active sites on the surface of the photocatalyst particles, 1.0 wt % NiO_x was also loaded on the surface of the photocatalyst particles from aqueous $Ni(NO_3)_2$ solution. The NiO_x-loaded photocatalysts were calcined at 500 °C in air for 1 h, and then reduced at 500 °C for 2 h in a mixed atmosphere of Ar and H_2 ($Ar/H_2 = 9:1$ by volume). Finally the H_2-treated photocatalysts were oxidized at 200 °C for 1 h in pure O_2 atmosphere in order to get the NiO/Ni bilayer structure on the

10.1021/jp0340919 CCC: $25.00
Published on Web 05/02/2003

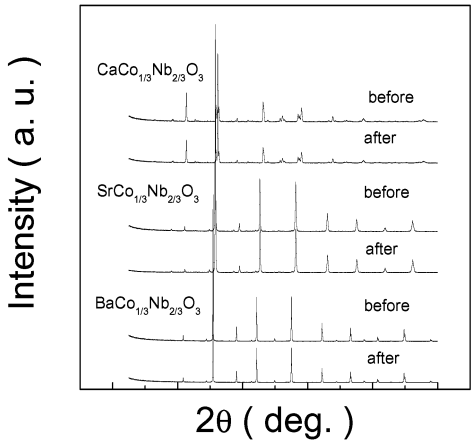

Figure 1. X-ray powder diffraction patterns for the photocatalysts $CaCo_{1/3}Nb_{2/3}O_3$, $SrCo_{1/3}Nb_{2/3}O_3$, and $BaCo_{1/3}Nb_{2/3}O_3$ before and after the H_2 evolution reaction from CH_3OH/H_2O solution.

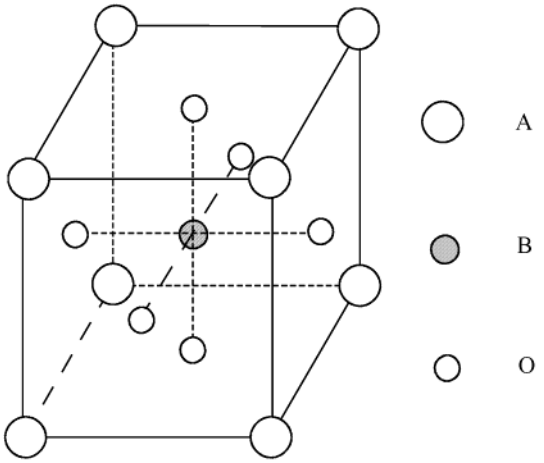

Figure 2. The schematic drawing of ABO_3 perovskite structure.

surface of the photocatalysts.[7] The surface areas of these compounds determined by the BET measurements are about 2.2 m^2/g.

3. Results and Discussion

3.1. Crystal Structural Analysis. Figure 1 shows X-ray powder diffraction patterns of $CaCo_{1/3}Nb_{2/3}O_3$, $SrCo_{1/3}Nb_{2/3}O_3$, and $BaCo_{1/3}Nb_{2/3}O_3$. $BaCo_{1/3}Nb_{2/3}O_3$ and $SrCo_{1/3}Nb_{2/3}O_3$ are well-crystallized with a simple cubic perovskite phase, while $CaCo_{1/3}Nb_{2/3}O_3$ is crystallized with a distorted monoclinic perovskite phase. For an ideal $A^{2+}B^{4+}O_3$-type perovskite structure, such as $CaTiO_3$, the corners of the cubic cell are occupied by A^{2+} ions with coordination number 12, and the sites of the face centers are occupied by O^{2-} ions with coordination number 6, while the bulk center is occupied by a B^{4+} ion with coordination number 6. B^{4+} and six neighboring O^{2-} ions form an octahedron BO_6, as schematically drawn in Figure 2. The neighboring octahedrons are connected to each other by sharing the corner to form a three-dimensional octahedron network. Here, for the perovskite compounds $CaCo_{1/3}Nb_{2/3}O_3$, $SrCo_{1/3}Nb_{2/3}O_3$ and $BaCo_{1/3}Nb_{2/3}O_3$, the site of the bulk center is occupied by Co^{2+} and Nb^{5+} ions randomly in a charge-balanced manner (CBM), which has been widely investigated in ferroelectric materials.[8,9] With the variation of the ionic radius of A^{2+} and B^{4+}, the crystal structure of ABO_3 perovskite will be subjected to some distortion, while the

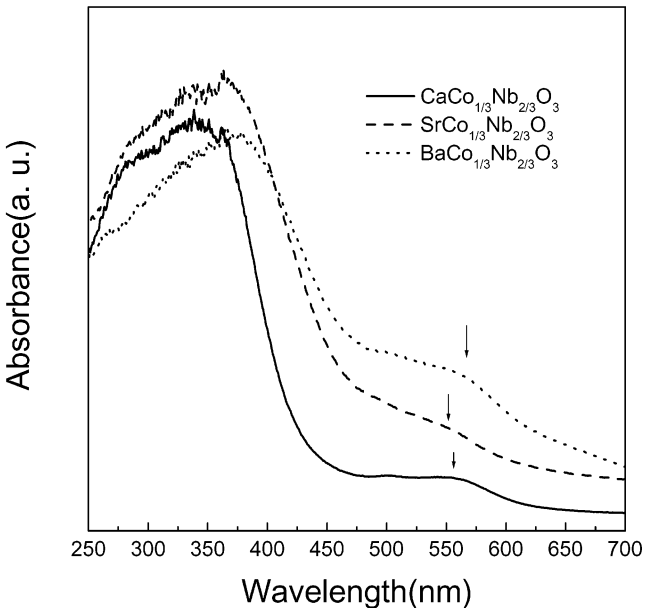

Figure 3. UV−vis diffuse reflectance spectra of the photocatalysts $CaCo_{1/3}Nb_{2/3}O_3$, $SrCo_{1/3}Nb_{2/3}O_3$, and $BaCo_{1/3}Nb_{2/3}O_3$.

TABLE 1: The Physical Properties and Lattice Parameters of the Photocatalysts $MCo_{1/3}Nb_{2/3}O_3$ (M = Ca, Sr, and Ba)

compound	structure	space group	tolerance factor	lattice parameter (nm)	band gap
$CaCo_{1/3}Nb_{2/3}O_3$	monoclinic	−	0.83	$a = 3.911$	
				$b = 3.892$	
				$c = 3.911$	
				$\beta = 91°16'$	2.80
$SrCo_{1/3}Nb_{2/3}O_3$	cubic	Pm3m	0.89	$a = 3.93$	2.46
$BaCo_{1/3}Nb_{2/3}O_3$	cubic	Pm3m	0.95	$a = 4.09$	2.46

following relationship among the radii of the three ions A^{2+}, B^{4+}, and O^{2-} exists:

$$r_A + r_O = t\sqrt{2}(r_B + r_O) \quad (1)$$

where t is defined as the tolerance factor. With the ionic radii of Ba^{2+}, Sr^{2+}, and Ca^{2+}, as listed in ref 10, the tolerance factors t of $BaCo_{1/3}Nb_{2/3}O_3$, $SrCo_{1/3}Nb_{2/3}O_3$, and $CaCo_{1/3}Nb_{2/3}O_3$ are estimated to be about 0.95, 0.89, and 0.83, respectively. The space group and lattice parameters for these compounds are listed in Table 1.

3.2. UV−vis Diffuse Reflectance Spectrum. Figure 3 shows UV−vis diffuse reflectance spectra of $CaCo_{1/3}Nb_{2/3}O_3$, $SrCo_{1/3}Nb_{2/3}O_3$, and $BaCo_{1/3}Nb_{2/3}O_3$ powders. We determined the band gaps of these compounds with the following equation as in refs 11,12:

$$\alpha = A((h\nu - E_g)^{n/2}/h\nu) \quad (2)$$

where α, ν, E_g, A, and n are the absorption coefficient, incident light frequency, band gap, constant, and an integer, respectively. The integer n depends on the characteristics of the optical transition ($n = 1$, 2, 4, and 6). The value of n as determined for $CaCo_{1/3}Nb_{2/3}O_3$, $SrCo_{1/3}Nb_{2/3}O_3$, and $BaCo_{1/3}Nb_{2/3}O_3$ is 2, indicating that the optical transitions as shown in Figure 3 for $CaCo_{1/3}Nb_{2/3}O_3$, $SrCo_{1/3}Nb_{2/3}O_3$, and $BaCo_{1/3}Nb_{2/3}O_3$ are directly forbidden.[12] The band gaps of $CaCo_{1/3}Nb_{2/3}O_3$, $SrCo_{1/3}Nb_{2/3}O_3$, and $BaCo_{1/3}Nb_{2/3}O_3$ are determined as about 2.80, 2.46, and 2.26 eV, respectively. With the variation of the ionic radius of Ba^{2+}, Sr^{2+}, and Ca^{2+}, the band gaps of these compounds change

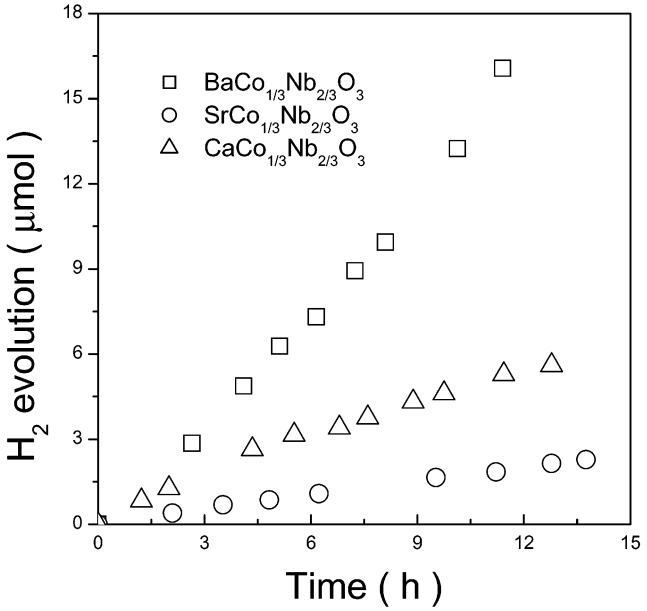

Figure 4. The formation rates of H_2 evolution from CH_3OH/H_2O solution with Pt cocatalyst under visible-light irradiation for the photocatalysts $CaCo_{1/3}Nb_{2/3}O_3$, $SrCo_{1/3}Nb_{2/3}O_3$, and $BaCo_{1/3}Nb_{2/3}O_3$(cat.: 0.5 g, Pt: 0.2 wt %, CH_3OH: 50 mL, H_2O: 220 mL, Xe arc lamp 300 W, $\lambda > 420$ nm).

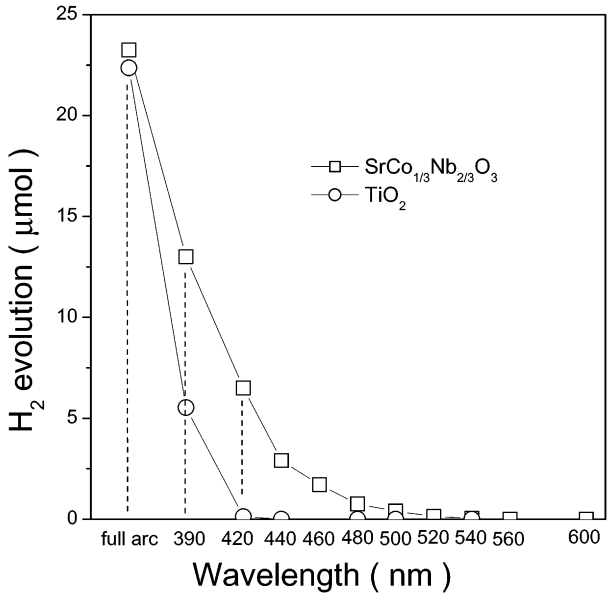

Figure 5. The wavelength dependence of H_2 formation rate from CH_3OH/H_2O solution with Pt cocatalyst in 10 hours for the photocatalyst $BaCo_{1/3}Nb_{2/3}O_3$ (cat: 0.5 g, Pt: 0.2 wt %, CH_3OH: 50 mL, H_2O: 220 mL, Xe arc lamp 300 W) and TiO_2 (P-25) (cat.: 0.1 g, Pt: 0.1 wt %, CH_3OH: 50 mL, H_2O: 220 mL, Xe arc lamp 300 W).

periodically. It is also obvious from Figure 3 that there is a hump on the right side of the reflectance spectrum of each compound, as shown by the arrow, which may be related to the other optical transitions in these compounds.

3.3. Photocatalytic Reactions under Visible-Light Irradiation. For a photocatalytic water-splitting process with a semiconductor, the following electrochemical requirements should be met: If the potential on the bottom of the conduction band is more negative than the redox potential of H^+/H_2 (0 V vs SHE, pH = 0), and the potential on the top of the valence band is more positive than the redox potential of O_2/H_2O (1.23 V vs SHE, pH = 0), the photogenerated electrons and holes will move to the surface of the photocatalyst and cause redox reactions. In our experiments, the easily oxidizable reducing reagent CH_3OH and electron acceptor $AgNO_3$ were employed to evaluate the photocatalytic activity of the photocatalysts $CaCo_{1/3}Nb_{2/3}O_3$, $SrCo_{1/3}Nb_{2/3}O_3$, and $BaCo_{1/3}Nb_{2/3}O_3$.

Figure 4 shows the formation rates of H_2 evolution from CH_3OH/H_2O solution with Pt cocatalyst (0.2 wt %) under visible-light irradiation ($\lambda > 420$ nm). With a rotative velocity 500 rpm, in the dark experiments no gas evolution from the mechano-catalysis process could be obtained for any sample, although it was reported that Co_3O_4 shows mechano-catalytic activity.[13] To identify the possibility that H_2 evolution for these compounds is from the contribution of the background of the system, a blank experiment was also performed, in which the reaction cell was only filled with 50 mL of CH_3OH, 220 mL of H_2O,and 0.2 wt % Pt cocatalyst without any photocatalyst powder under visible-light irradiation ($\lambda > 420$ nm). No gas evolution could be obtained during the blank experiment. Moreover, the wavelength dependence of H_2 formation rate from CH_3OH/H_2O solution with 0.2 wt % Pt cocatalyst for 0.5 g $BaCo_{1/3}Nb_{2/3}O_3$ in 10 hours was investigated with a quartz cell by using different cutoff filters, as shown in Figure 5. For making a comparison, the wavelength dependence of H_2 formation rate from CH_3OH/H_2O solution with 0.1 wt % Pt cocatalyst in 10 hours for 0.1 g TiO_2 (P-25) is also drawn in Figure 5. From Figure 5, the photocatalytic activity of TiO_2 could not be observed under visible-light irradiation $\lambda > 420$ nm), while an obvious photocatalytic activity could be obtained on $BaCo_{1/3}Nb_{2/3}O_3$. When the wavelength of the cutoff filter is larger than 540 nm, almost no gas evolution could be observed. This is in agreement with the UV−vis diffuse reflectance spectrum of $BaCo_{1/3}Nb_{2/3}O_3$. The results of the above experiments mean that the photocatalytic activities of the photocatalysts $CaCo_{1/3}Nb_{2/3}O_3$, $SrCo_{1/3}Nb_{2/3}O_3$, and $BaCo_{1/3}Nb_{2/3}O_3$, as observed in our experiments under visible-light irradiation, should be ascribed to the visible-light absorption.

TABLE 2: Photocatalytic Activities of $MCo_{1/3}Nb_{2/3}O_3$ (M = Ca, Sr, and Ba)

compound	co-catalyst	condition of water	activity (H_2) (μmol/h)
$CaCo_{1/3}Nb_{2/3}O_3$	Pt	50 mL CH_3OH	0.44
	NiO_x	pure water	0.86
$SrCo_{1/3}Nb_{2/3}O_3$	Pt	50 mL CH_3OH	0.17
	NiO_x	pure water	0.86
$BaCo_{1/3}Nb_{2/3}O_3$	Pt	50 mL CH_3OH	1.4
	NiO_x	pure water	1.37

As listed in Table 2, the following sequence of the photocatalytic activity in evolving H_2 from CH_3OH/H_2O solution for these compounds under visible-light irradiation could be obtained:

$$\text{Rate}_{BaCo_{1/3}Nb_{2/3}O_3} > \text{Rate}_{CaCo_{1/3}Nb_{2/3}O3} > \text{Rate}_{SrCo_{1/3}Nb_{2/3}O_3} \quad (3)$$

with the decrease of the ionic radius from Ba^{2+} to Sr^{2+}, the lattice parameter of $SrCo_{1/3}Nb_{2/3}O_3$ is shortened, thus leading to a larger band gap resulting from a relationship between the band gap E_g and the lattice parameter a for a cubic perovskite structure: $E_g \propto (1/a^2)$. Although generally the wide band gap for a series of semiconductors with the same crystal symmetry means higher photocatalytic activity under UV-light irradiation such as titanate,[14] here just a reversed result is obtained for $BaCo_{1/3}Nb_{2/3}O_3$ and $SrCo_{1/3}Nb_{2/3}O_3$ under visible-light irradiation. This can be ascribed to the following aspects. Due to the cutoff filter (420 nm) as employed, the smaller band gap of $BaCo_{1/3}Nb_{2/3}O_3$ means a larger quantum of the absorbed photons

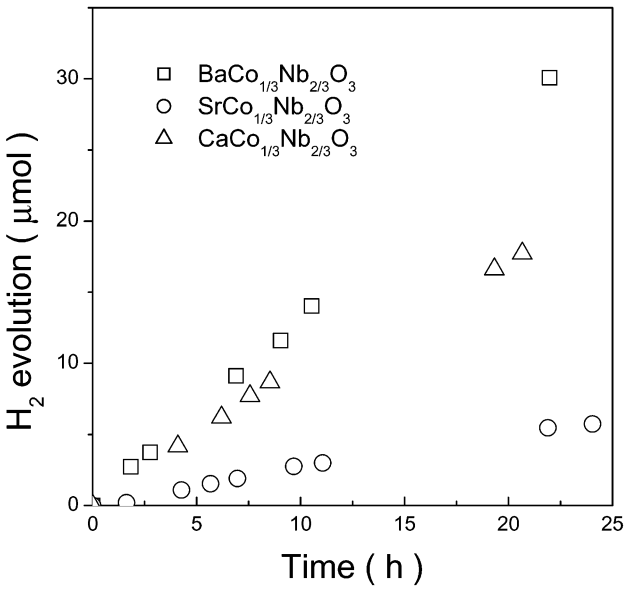

Figure 6. The formation rates of H_2 evolution from pure water with the NiO_x-loaded $CaCo_{1/3}Nb_{2/3}O_3$, $SrCo_{1/3}Nb_{2/3}O_3$, and $BaCo_{1/3}Nb_{2/3}O_3$ photocatalyst particles under visible-light irradiation (cat.: 0.5 g, NiO_x: 1.0 wt %, H_2O: 270 mL, Xe arc lamp 300 W, $\lambda > 420$ nm).

of visible light, indicating more photogenerated electron−hole pairs moving to the surface of the photocatalyst, thus leading to higher photocatalytic activity. With the smallest ionic radius in the A site, $CaCo_{1/3}Nb_{2/3}O_3$ shows monoclinic crystal structure, different from that of $BaCo_{1/3}Nb_{2/3}O_3$ and $SrCo_{1/3}Nb_{2/3}O_3$, so it shows a special photocatalytic activity. O_2 evolution from $AgNO_3$ solution for these compounds was also obtained, while the reaction process was complicated. Further investigation on the reaction will be performed later.

Figure 6 shows the formation rates of H_2 evolution from pure water with the NiO_x-loaded $CaCo_{1/3}Nb_{2/3}O_3$, $SrCo_{1/3}Nb_{2/3}O_3$, and $BaCo_{1/3}Nb_{2/3}O_3$ photocatalyst particles under visible-light irradiation ($\lambda > 420$ nm). The same sequence of the photocatalytic activity as inequality (eq 3) could be observed for the photocatalysts $CaCo_{1/3}Nb_{2/3}O_3$, $SrCo_{1/3}Nb_{2/3}O_3$, and $BaCo_{1/3}Nb_{2/3}O_3$. In a prolonged experiment (145 h) for $BaCo_{1/3}Nb_{2/3}O_3$ photocatalyst, about 164 μmol of H_2 was obtained, and the turnover number of the reacted electrons to the amount of Ni loaded on the surface of the sample reached 5. This means that the reaction of H_2 evolution occurs catalytically. During these experiments, no O_2 evolution could be found for any sample. It may be related to the physisorbed and chemisorbed states of O_2 molecules on the surface of the photocatalyst particles, just as found on TiO_2.[15,16] A series of the diffusions of these physisorbed and chemisorbed oxygen molecules along or over the crystalline boundaries also may be responsible for the "absent" oxygen.[17]

4. Suggested Model of Electronic Structures

The electronic structure of the transition-metal oxide with perovskite structure is generally defined by the d-level of the transition metal and the 2p-level of the ligand O atom,[18,19] when the d orbitals of the transition metal are empty. While for the transition-metal oxide with the d orbitals partially occupied, the electronic structure formed is under the strong influence of the anisotropic crystal fields of the octahedron formed by the transition metal and the ligand O atoms. The 3d orbitals show a 10-fold degeneracy due to their total angular momentum L = 2. This degeneracy will be lifted by the anisotropic crystal field. The cubic lattice symmetry leads to an higher energy level of 4-fold degenerate e_g orbitals and 6-fold degenerate lower orbitals t_{2g}. For the monoclinic lattice symmetry, above e_g, orbitals with 4-fold degeneracy will be further split into a higher-energy $d_{x^2-y^2}$ orbital and a lower-energy d_{z^2} orbital, while a t_{2g} orbital with 6-fold degeneracy will be further split into three discrete sub-orbitals: d_{xy}, d_{yz}, and d_{xz}. Thus, for Co^{2+} with the electronic configuration $3d^7$ in the photocatalysts $BaCo_{1/3}Nb_{2/3}O_3$ and $SrCo_{1/3}Nb_{2/3}O_3$ with the cubic crystal symmetry, the following electronic occupying states should be expected: t_{2g} orbitals are fully occupied, and e_g orbitals are partially occupied. For Co^{2+} in the photocatalyst $CaCo_{1/3}Nb_{2/3}O_3$ with monoclinic crystal symmetry, the following electronic occupying states should be expected: the sub-orbitals d_{xy}, d_{yz}, and d_{xz} are fully occupied, and the sub-orbital d_z^2 is partially occupied, while sub-orbital $d_{x^2-y^2}$ is empty. To have a simple model, here we supposed that Co^{2+} in these compounds has a low spin state ($t_{2g}{}^6t_{2g}{}^3e_g{}^1$), although it was reported that Co^{3+} in some cobalt oxides possibly shows low-spin state ($t_{2g}{}^6t_{2g}{}^3$), intermediate-spin state ($t_{2g}{}^5t_{2g}{}^2e_g{}^1$), and high-spin state ($t_{2g}{}^4t_{2g}{}^2e_g{}^2$).[20] $CaCo_{1/3}Nb_{2/3}O_3$, $SrCo_{1/3}Nb_{2/3}O_3$, and $BaCo_{1/3}Nb_{2/3}O_3$ behave as a semiconductor, because the electrons occupying sub-orbital d_z^2 are localized. So it is reasonably concluded that the band structures of $CaCo_{1/3}Nb_{2/3}O_3$, $SrCo_{1/3}Nb_{2/3}O_3$, and $BaCo_{1/3}Nb_{2/3}O_3$ should be

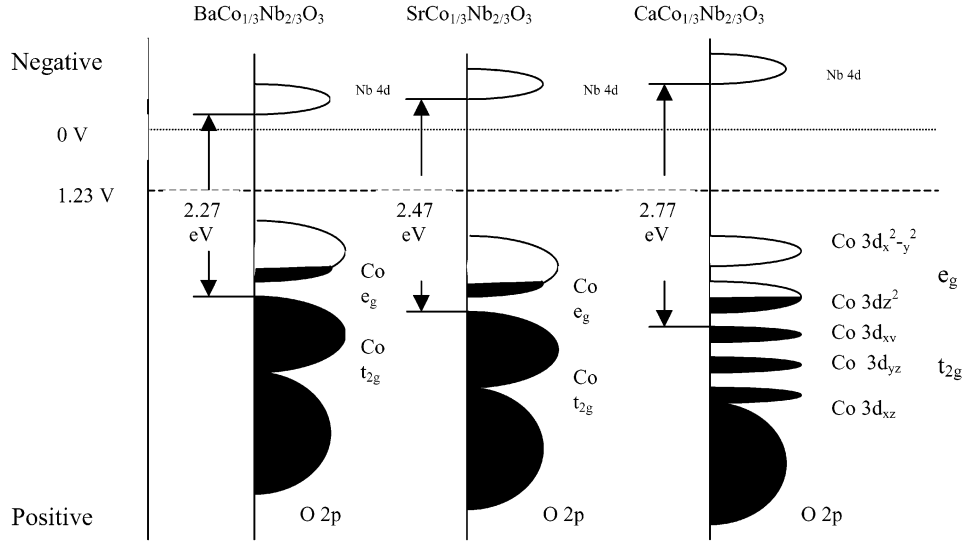

Figure 7. The suggested model of the electronic structures for the photocatalysts $CaCo_{1/3}Nb_{2/3}O_3$, $SrCo_{1/3}Nb_{2/3}O_3$, and $BaCo_{1/3}Nb_{2/3}O_3$.

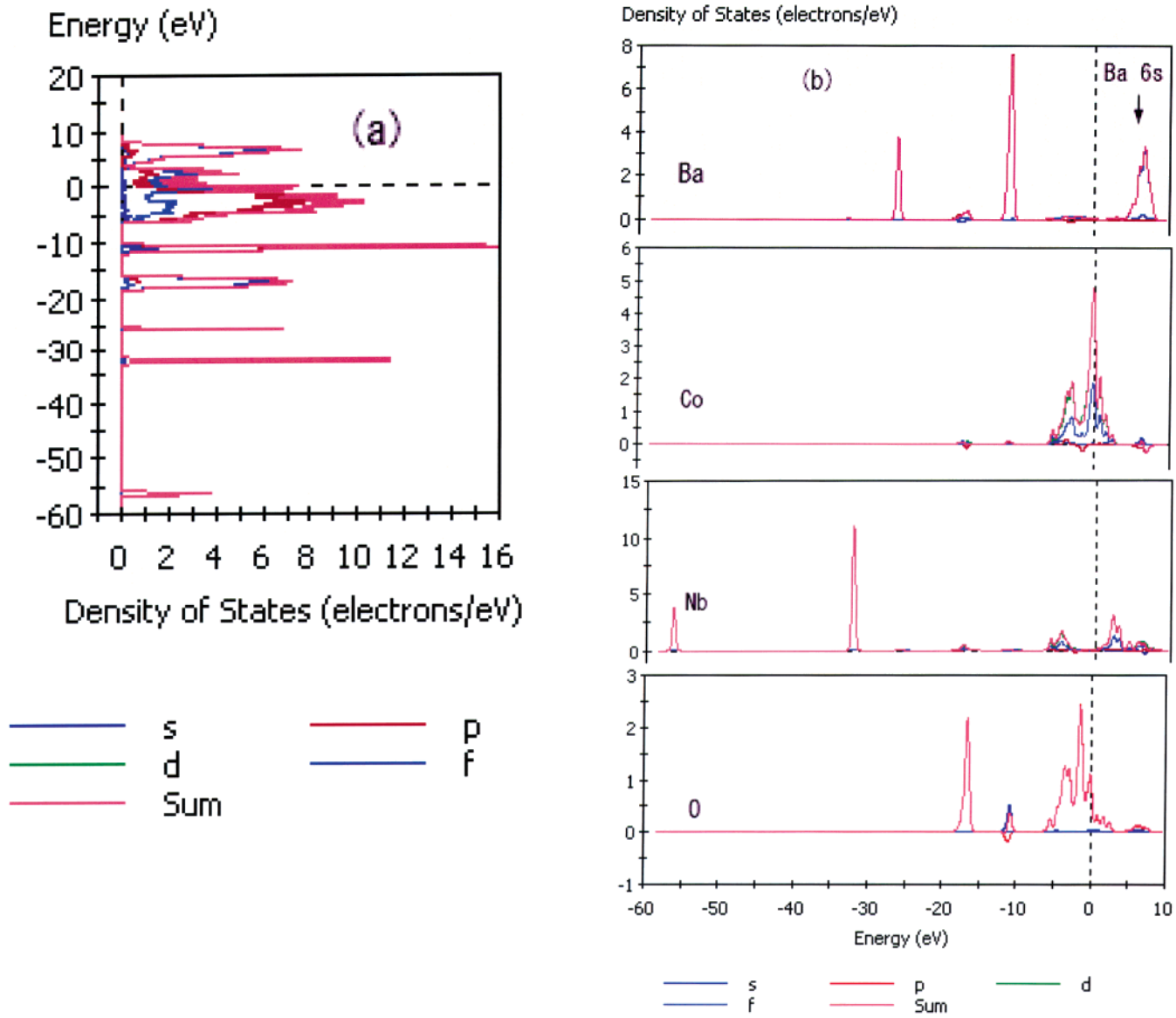

Figure 8. The projected total(a), and partial(b) density of states(DOS) for $BaCo_{1/3}Nb_{2/3}O_3$.

composed of the Co^{2+} 3d level (t_{2g} or e_g) and the Nb^{5+} 4d level. The schematic model of the electronic structures for the photocatalysts $CaCo_{1/3}Nb_{2/3}O_3$, $SrCo_{1/3}Nb_{2/3}O_3$, and $BaCo_{1/3}Nb_{2/3}O_3$ are drawn in Figure 7. The observed visible-light absorptions in Figure 3 for $CaCo_{1/3}Nb_{2/3}O_3$, $SrCo_{1/3}Nb_{2/3}O_3$, and $BaCo_{1/3}Nb_{2/3}O_3$ should be ascribed to the electronic excitations from the Co^{2+} t_{2g} state to the Nb^{5+} 4d state. The humps on the right side of Figure 3 for these compounds should be ascribed to the electronic excitation from the Co^{2+} e_g state to the Nb^{5+} 4d state. This later optical absorption also may be responsible for the high background of the UV−vis diffuse reflectance spectra in the region of long wavelength.

5. First Principles Theory Calculation

With the data of the crystal structure of $BaCo_{1/3}Nb_{2/3}O_3$, as listed in Table 1, the electronic structure of $BaCo_{1/3}Nb_{2/3}O_3$ was studied by the F-LAPW method (Materials Studio∼CASTEP, Accelrys Inc). Because the atom positions for $CaCo_{1/3}Co_{2/3}O_3$ are unknown up to now, the theoretical calculation of the electronic structure has not been performed. Figures 8a and 8b show the projected partial and total density of states (DOS) for $BaCo_{1/3}Nb_{2/3}O_3$. The Co^{2+} 3d band is split into two main peaks: the lower part is t_{2g} states and the higher part is e_g states. In addition, the Co^{2+} 3d states heavily overlap with the O 2p states. It means that the Co^{2+} 3d states are strongly hybridized with the O 2p states. So, in the CoO_6 octahedron, the O−Co−O bond is mainly covalent. It is similar to that observed in other perovskite compounds containing Co^{3+} ions, such as $LaCoO_3$.[21] It is also obvious from Figure 8 that the Nb^{5+} 4d states overlap with the O 2p states a little, indicating that in a NbO_6 octahedron the O−Nb−O bond is mainly ionic. The difference between the bonds of O−Co−O and O−Nb−O is ascribed to their special electronegativity (1.6, 1.88, and 3.44 for Nb, Co, and O, respectively).

6. Conclusion

In summary, we have developed a new series of the visible-light-driven photocatalysts $MCo_{1/3}Nb_{2/3}O_3$ (M = Ca, Sr, and Ba) with an ABO_3-type perovskite structure, in which the B site is occupied by Co^{2+} and Nb^{5+} randomly. With the variation of the radius from Ca to Ba, the band gaps of the compounds $CaCo_{1/3}Nb_{2/3}O_3$, $SrCo_{1/3}Nb_{2/3}O_3$, and $BaCo_{1/3}Nb_{2/3}O_3$ become narrower, while the photocatalytic activities of these compounds under visible-light irradiation show no periodic sequence due

to the special crystal symmetry of $CaCo_{1/3}Nb_{2/3}O_3$. It is suggested that the valence bands of these compounds are composed of the Co^{2+} 3d states, and the conduction bands are composed of the Nb 4d states. The theoretical calculation of the electronic structure for $BaCo_{1/3}Nb_{2/3}O_3$ shows that the bond O−Co−O is mainly covalent, while the bond O−Nb−O is mainly ionic.

Although the photocatalytic activities of these compounds under visible-light irradiation are not very high at present, they may be made promising visible-light-driven photocatalysts by modifying their surface conditions and increasing their surface area.

Acknowledgment. One of the authors thanks JSPS fellowship for financial support.

References and Notes

(1) Fujishima, A.; Honda, K. *Nature (London)* **1972**, *238*, 37.
(2) Asahi, R.; Morikawa, T.; Ohwaki, T.; Aoki, K.; Taga, Y. *Science* **2001**, *293*, 269.
(3) Zou, Z.; Ye, J.; Sayama, K.; Arakawa, H. *Nature(London)* **2001**, *414*, 625.
(4) Geoffrey, B. S.; Thoms, E. M. *J. Phys. Chem. B* **1997**, *101*, 2508.
(5) Kudo, A.; Kato, H.; Nakagawa, S. *J. Phys. Chem. B* **2000**, *104*, 571.
(6) Hitoki, G.; Ishikawa, A.; Takata, T.; Kondo, J.; Hara, M.; Domen, K. *Chem. Lett.* **2002**, 736.
(7) Domen, K.; Kudo, A.; Onishi, T. *J. Catal.* **1986**, *102*, 92.
(8) Gao, X. S.; Chen, X. Y.; Yin, J.; Wu, J.; Liu, Z. G. *J. Mater. Sci.* **2000**, *35*, 5421.
(9) Goodenough, J. B.; Lango, J. M. Landolt-Boornstein Tabellen, New series. Springer: Berlin, 1970; Vol. III/4a.
(10) Lide, D. R. *Handbook of Chemistry and Physics*, 80th ed. 1999−2000; CRC Press LLC: Boca Raton, FL, 1999.
(11) Yin, J.; Zou, Z.; Ye, J. *J. Mater. Res.: Rapid Commun.* **2002**, *17* (9).
(12) Butler, M. A. *J. Appl. Phys.* **1977**, *48*, 1914.
(13) Domen, K.; Kondo, J. N.; Hara, M.; Takata, T. *Bull. Chem. Soc. Jpn.* **2000**, *73*, 1307.
(14) Oosawa, Y.; Takahashi, R.; Yonemura, M.; Sekine, T.; Goto, Y. *New J. Chem.* **1989**, *13*, 435.
(15) Yanagisawa, Y.; Ota, Y. *Surf. Sci.* **1991**, *254*, L433.
(16) Lu, G.; Amy, L.; Yates, J. T., Jr. *Chem. Rev.* **1995**, *102*, 3005.
(17) Svensson, A. M.; Sunde, S.; Nisancioglu, K. *J. Electrochem. Soc.* **1998**, *145*, 1390.
(18) Scaife, D. E. *Solar Energy* **1980**, *25*, 41.
(19) Arima, T.; Tokura, Y. *Phys. Rev. B* **1993**, *48*, 17006.
(20) Ravindran, P.; Korzhavyi, P. A.; Fjellvag, H.; Kjekshus, A. *Phys. Rev. B* **1999**, *60*, 16423.
(21) Takahashi, H.; Munakata, F.; Yamanaka, M. *Phys. Rev. B* **1996**, *53*, 3731.